

An alternative wind profile formulation for urban areas in neutral conditions

Armando Pelliccioni¹, Paolo Monti² and Giovanni Leuzzi²

¹INAIL-DIPIA, Via Fontana Candida 1, 00040 Monteporzio Catone, Roma (Italy)

²DICEA, Università di Roma “La Sapienza”, Via Eudossiana 18, 00184 Roma (Italy)

Corresponding author:

Paolo Monti. Tel: 00390644585045. Fax: 00390644585065; E-mail: paolo.monti@uniroma1.it

Abstract

On the basis of meteorological observations conducted within the city of Rome, Italy, a new formulation of the wind-speed profile valid in urban areas and neutral conditions is developed. It is found that the role played by the roughness length in the canonical log-law profile can be taken by a local length scale, depending on both the surface cover and the distance above the ground surface, which follows a pattern of exponential decrease with height. The results show that the proposed model leads to increased performance compared with that obtained by using other approaches found in the literature.

Key words: MOST; roughness length; wind profile; urban boundary layer, roughness sublayer; inertial sublayer.

1. Introduction

Aerodynamic roughness (buildings and other structures), moisture availability and radiative and thermal properties (albedo, emissivity, heat capacity, thermal conductivity, among others) differentiate urban areas from their rural surroundings. This leads to the formation of a region defined as the urban boundary layer (UBL) [10, 22]. The analysis of the UBL, which is in general horizontally inhomogeneous and strongly dependent on the height, is complicated by the presence of internal boundary layers within internal boundary layers [12, 23], each of them with its own thermal and dynamical characteristics (as reviewed by Britter and Hanna [5]). A consequence is the need to develop alternative approaches to the classical similarity theory for flow modeling in urban complexes. To this end, the case of neutral atmosphere is the first step for any successive analysis in diabatic conditions.

One of the problems encountered in UBL studies is that the canonical Monin-Obukhov similarity theory (MOST), does not hold in that it is strictly valid for flat terrain only. For neutrally stratified UBLs, the mean horizontal velocity u as a function of the height z is usually described by the classical log-law [30]:

$$u(z) = \frac{u_*}{k} \ln \left[\frac{z-d_0}{z_0} \right] \quad (1)$$

where z_0 is the roughness length, d_0 the displacement height, u_* the friction velocity and $k=0.4$ the von Karman constant. Equation (1) should be valid in the constant flux or inertial sublayer (ISL) overlying the roughness sublayer (RSL), i.e. the portion of atmosphere immediately above the urban canopy [5]. The RSL includes the height range in which the flow is strongly influenced by the roughness elements (buildings and vegetation) and the determination of its depth in terms of buildings height or other physical parameters is not a simple task [8, 29].

In flat terrain (i.e. $d_0=0$) the roughness length can easily be estimated from well-known land-use categories [30] or in terms of the Reynolds number [11] and the Rossby number [31]. In urban canopies, z_0 and d_0 can be obtained by using morphometric methods (among others Macdonald et al. [20], hereinafter MGH98; Grimmond and Oke [13], hereinafter GO99; Di Sabatino et al. [9]). In the case of neutral atmosphere, Kastner-Klein and Rotach [17] (hereinafter KR04) estimated z_0 and d_0 using morphometric methods and calculated u_* from Eq. (1), while Cheng and Castro [6] (hereinafter CC02) calculated z_0 and d_0 starting from the measured shear stresses profile. More recently, Harman and Finnigan [14] developed profile functions, tested in vegetated canopies, which do not show discontinuity at the interface between RSL and ISL. In particular, they found a relationship for the

vertical profile of the wind speed that is comprised of a canopy model coupled to a modified surface-layer model, formulated through the mixed layer analogy for the flow at a canopy top. In essence, their model consists of an extension of the canonical log-law where the influence of the RSL is taken into account by introducing an additional function.

In an attempt to develop improved models for the wind-speed profile in urban areas for neutral conditions, we propose here a new formulation where the role played by the roughness length, i.e. the constant of integration of the vertical gradient of the wind-speed, is taken by a new “variable” quantity. Advanced analysis on the common meaning of z_0 and the procedure for its calculation can be found in the literature since the early 1970s. To our knowledge, Arya [3] was the first to consider that the roughness height could depend on stratification. More recently, Zilitinkevich et al. [32] showed that the atmospheric stability strongly affects z_0 , especially for the stable case, where z_0 monotonically decreases as stability becomes stronger. Barlow et al. [4] found from observations taken in Salford, UK, a logarithmic layer up to 65 m height, while at higher elevations the velocity showed a different vertical gradient because of the presence of a change in surface cover upstream of the measurement station. Similarly, Li et al. [18] observed the presence of kinks at 100 m and 200 m levels in the vertical velocity profiles taken at Beijing, China. They argued that such abrupt variations could be attributed to the influence of the changes in surface roughness from suburban to urban terrain. From analysis of wind profiles taken at Uppsala, Sweden, Karlsson [16] found an apparent roughness length which was allowed to adjust to the different vertical layers (lower and upper layers) and atmospheric stability. Experimental analysis conducted in the same urban complex considered in the present study [25] reveals that, at least for neutral conditions, the optimal value of z_0 to be inserted in Eq. (1) decreases with height. At elevated layers, z_0 tend to values close to those listed in typical urban land use categories.

Based on these last results, we conjectured that z_0 may not be treated as a constant entity but as a variable parameter, the value of which might depend on both the flow characteristics and the height. An investigation is therefore presented here with the purpose to propose a relationship for the wind profile in the UBL - in neutral conditions - where the assumption of constant z_0 is removed.

The analysis is conducted using a set of meteorological data taken from a site located within the city of Rome, Italy. Wind and temperature profiles taken from ground level ($z=0$) up to 200 m during one year by means of a RASS/SODAR system are used for the analysis together with data acquired close to the surface using a conventional meteorological station. The following section describes the field

campaign. Section 3 reports the conceptual description of the proposed model, while Section 4 is devoted to the model evaluation. Conclusions are given in Section 5.

2. Datasets

The dataset refers to a field campaign conducted at the Villa Pamphili urban park (VP), a site located within the city of Rome, Italy, during the period June 2005-July 2006. That large feature (Fig. 1), situated in the west part of the city, ($41^{\circ}53'N$, $12^{\circ}26'E$), interrupts built-up zones. Local circulations with a pronounced diurnal cycle are usually predominant in that area for the most part of the year [2, 19, 21, 27]. The measurements were made away from buildings and trees (blue dot in Fig. 1) and hence the data can be considered as free from the immediate effects of obstacles.

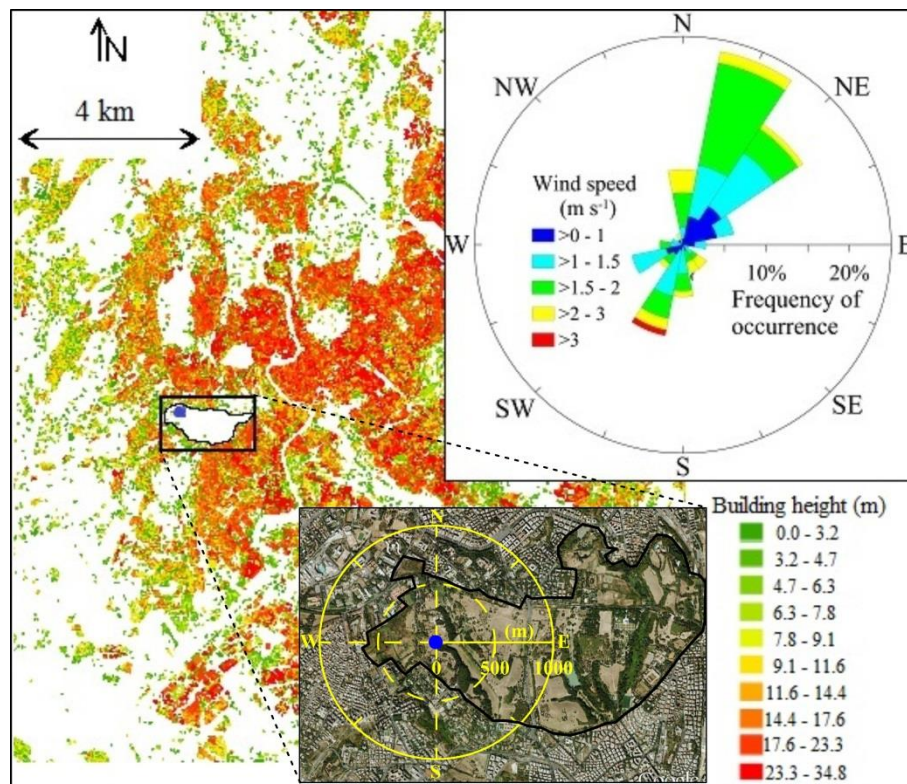


Fig. 1 Rome area. Colors are building heights. The black line within the rectangle indicates VP park, while the blue circle at the north-west part of VP refers to the location of the meteorological site. The inset (aerial picture produced using Google Earth) shows the enlargement of VP park. The wind rose calculated during neutral conditions using the ultrasonic anemometer at $z=10$ m is also shown

The meteorological instruments included a 10 m mast equipped with two triaxial ultrasonic anemometers (GILL Windmaster, sampling rate equal to 4 Hz) mounted at $z=5.5$ m and $z=10$ m above

the ground level. Two thermistors (Vaisala PT1000) placed at $z=1.6$ m and $z=10$ m provided measurements of the air temperature. Note that the acquisition frequency (4 Hz) of the ultrasonic anemometers is quite low compared to that generally used for measurements of turbulent variables (≥ 10 Hz). This might lead to underestimation of both statistical moments and eddy fluxes.

A SODAR/RASS system (Metek, model DSPA90) was used to measure the three components of the wind velocity and the virtual air temperature from $z=40$ m up to $z=400$ m with a resolution of 20 m. The system provided the vertical profiles of velocity and temperature averaged every 10 min. Since the analysis regards the neutral boundary layer, a stringent criterion to select neutral conditions was adopted in order to minimize inaccuracies related to possible uncertainties in the estimation of the Obukhov length $L = -u_*^3(kq_0)^{-1}$, used as an indicator of the flow stability (q_0 is the kinematic heat flux). In particular, only the vertical profiles corresponding to $|z/L| \leq 0.01$ were considered as representative of the statically neutral UBL. Here $z=10$ m, i.e. the height of the top ultrasonic anemometer used to calculate u_* . As both the ultrasonic anemometers and the thermometers used in the campaign did not give information on the temperature fluctuations, no directly measured heat flux q_0 was available. This quantity may be estimated to reasonable precision based on the first order closure of the turbulence and temperature measured by the two thermistors (information on q_0 estimation and further details on the field campaign can be found in Pelliccioni et al. [25]).

Given that during neutral conditions the distribution of the wind direction observed at VP was characterized by the N-NE direction (see wind rose in Fig. 1), in what follows only events of winds coming from that sector ($22.5^\circ \pm 11.25^\circ$) are considered. Such a sector corresponds to a highly urbanized area, where the most representative building height H was nearly 18 m. Finally, only the profiles that obey the condition of quasi-constancy of the wind direction along the vertical were retained. In particular, the vertical profile is discarded if the variation of wind direction in the range $10 < z < 200$ m is greater than 22.5° . In this way, 36 profiles were selected for the analysis. This is a concession to the requirement that the analysis is robust.

3. The local length scale

As a first step, we suppose that the length scale z_0 which appears in the canonical log-law based on MOST, i.e. $u(z) = (u_*/k)\ln[z/z_0]$, is a quantity which depends not only on the surface characteristics but also on the height. As a consequence, we can introduce a new variable, $z_{0L}(z)$, which assumes the meaning of *local* length scale. Given wind speed observations in neutral conditions at several heights, one can define z_{0L} simply by substitution of z_0 by z_{0L} :

$$u(z) = \frac{u_*}{k} \ln \left[\frac{z}{z_{0L}(z)} \right] \quad (2)$$

Assuming u_* measured at a reference height, z_{ref} , Eq. (2) gives:

$$z_{0L}(z) = \frac{z}{\exp \left[\frac{u(z) \cdot k}{u_*(z_{\text{ref}})} \right]} \quad (3)$$

This procedure is generally used for calculating the (constant) values of z_0 and d_0 from Eq. (1) given the wind speed taken at two or more levels within the surface layer, where u_* does not vary with height [30]. Nevertheless, as will be shown below, the analysis of the wind profiles taken at VP suggests that z_{0L} varies much with height even when u_* does not. Thus, we extend the use of the MOST even to the cases where it is not strictly valid.

3.1 Experimental evidence

Following the considerations above, we calculated $z_{0L}(z)$ for each vertical profile of the VP dataset using Eq. (3) and assuming $z_{\text{ref}}=10$ m (the location of the ultrasonic anemometer). The average profiles of $z_{0L}(z)$ were grouped into 4 classes of $u_*(z_{\text{ref}})$, centred on the values 0.35, 0.44, 0.53 and 0.64 m s^{-1} defined on the basis of the range of values calculated for $u_*(z_{\text{ref}})$ during the campaign. A fifth class referred to the value of the friction velocity averaged over all the 36 events, $u_*(z_{\text{ref}}) = 0.49 \text{ m s}^{-1}$, was also used for the analysis.

Figure 2a shows the average profiles of z_{0L} as a function of the non-dimensional height z/H . With the exclusion of the outlier data point obtained at $z=10$ m for $u_*(z_{\text{ref}}) = 0.35 \text{ m s}^{-1}$, z_{0L} is larger at low levels, nearly 3 m, irrespective of $u_*(z_{\text{ref}})$. Moreover, the larger average $u_*(z_{\text{ref}})$ the larger z_{0L} . As height increases z_{0L} decreases until it reaches a minimum close to 0.5 m at $z/H=11.1$. Note that for $z/H \geq 6.6$, z_{0L} is nearly constant and hence the classical log-law with constant roughness length holds. This suggests that an ISL should be present therein, while that is not true for $z/H \leq 6.6$.

As pointed out by Andreas et al. [1], the variability of u_* with height is somewhat unimportant for the existence of the log-law in flat terrain for neutral conditions. This seems to be true also for the VP site. However, to verify whether the vertical variation of z_{0L} could be ascribed to vertical variations of u_* or not, we calculated $u_*(z)$ in an indirect way using the vertical profile of the measured standard

deviation of the vertical velocity $\sigma_w(z)$ (the SODAR system does not give information about the friction velocity). In particular, $u_*(z)$ can be estimated, in the case of flat terrain and neutral conditions, from the relation $u_*(z) = a \cdot \sigma_w(z)$, where a is a constant [24]. It follows that:

$$\frac{u_*(z)}{u_*(z_{ref})} = \frac{\sigma_w(z)}{\sigma_w(z_{ref})} = R(z) \quad (4)$$

which gives the vertical profile of $u_*(z)$ from u_* measured by the sonic anemometer at z_{ref} and from $\sigma_w(z)$ acquired along z by the SODAR, viz.:

$$u_*(z) = \frac{u_*(z_{ref})}{\sigma_w(z_{ref})} \sigma_w(z) = R(z) \cdot \sigma_w(z) \quad (5)$$

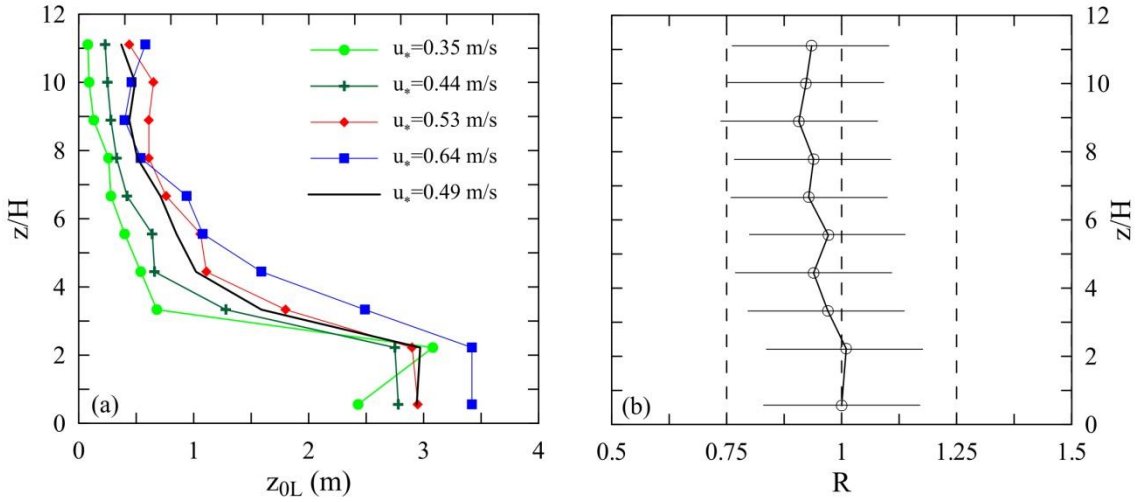


Fig. 2 (a) Vertical profiles of the averaged z_{0L} for classes of u_* . (b) Vertical profile of the ratio $R(z/H) = u_*(z/H) / u_*(z_{ref}=10 \text{ m})$. Note that the lower data point refers to the sonic anemometer. The error bar gives sample standard deviation

Figure 2b shows R , calculated irrespective of the class of $u_*(z_{ref})$, as a function of z/H . It decreases slightly with z/H and is about unity for $z/H \leq 5.5$. Thus, u_* decreases little with height too (its value at $z/H=11.1$ is nearly 90% the surface value) and hence a layer of quasi-constant mechanical flux above the surface seems to exist. Since the footprint analysis performed by [25] suggests that the flow at VP is strongly affected by the city, this means that a RSL is present and that u_* is nearly-constant therein. Therefore, the classical log-law with constant roughness length might be invalid in that portion of the UBL even if a quasi-constant flux layer is present. Similar results were obtained by Pelliccioni

et al. [26] who analyzed vertical profiles of u_* , taken in correspondence of an urban area, available in the CEDVAL dataset (compilation of wind tunnel datasets provided by the Environmental Wind Tunnel Laboratory of the Meteorological Institute of Hamburg University, see for example [15]). In particular, Pelliccioni et al. [26] found that under certain circumstances the classical log-law does not hold for $z/H \leq 3$ even though a quasi-constant flux layer exists, similarly to what was observed by Dallman et al. [7] in a suburban/industrial area. The accordance with what we observed at VP is less evident (the log-law is not valid at VP for $z/H \leq 6.6$). This discrepancy is perhaps reflective of the different characteristics of the land use upwind the measurement sites.

3.2 Theoretical interpretation

On the basis of the experiments reported in the previous sub-section, we may derive a suitable function $z_{0L}(z)$, bearing in mind that it might depend also on the flow. In this context, the canonical roughness length should be considered as a zero-order approach, viz.:

$$\frac{dz_{0L}}{dz} = 0 \quad (6)$$

from which results $z_{0L}=z_0=\text{const}$. In a first-order approach, the right hand side of Eq. (6) is no longer zero, but is a function whose expression is not straightforward. With the constraint of a simple form for z_{0L} , the first order approach with respect to Eq. (6):

$$\frac{dz_{0L}}{dz} = \beta' z_{0L} + \gamma' \quad (7)$$

seems to be a reasonable choice. This closure leads to the zero-order Eq. (6) when $\beta'=\gamma'=0$. By integrating Eq. (7) one obtains:

$$\int_{z_{0S}}^{z_{0L}} \frac{dz_{0L}}{\beta' z_{0L} + \gamma'} = \int_0^z dz \quad (8)$$

where $z_{0S} = z_{0L}|_{z=0}$. Solving Eq. (8), one obtains:

$$z_{0L}(z) = \left(z_{0S} + \frac{\gamma'}{\beta'} \right) \cdot \exp[\beta' \cdot z] - \frac{\gamma'}{\beta'} \quad (9)$$

After making the change of variables $\alpha=z_{0S}+\gamma'/\beta'$, $\beta=-\beta'$ and $\gamma=\gamma'/\beta'$, one obtains a functional form of $z_{0L}(z;\alpha,\beta,\gamma)$ totally equivalent to Eq. (9):

$$z_{0L}(z) = \alpha \cdot \exp[-\beta \cdot z] + \gamma \quad (10)$$

The quantity β can be viewed as the inverse of a length scale, $L_C=1/\beta$, which has the role of incorporating the effects of the roughness elements on the undisturbed flow and, therefore, on the local length scale. Its value is connected to the complexity of the surface (from a geometrical point of view) and might be considered related to the RSL height. Introducing L_C in Eq. (10) one gets the formulation of the vertical profile of z_{0L} :

$$z_{0L}(z) = \alpha \cdot \exp\left[-\frac{z}{L_C}\right] + \gamma \quad (11)$$

which shows that the local length scale consists of two parts: one takes into account the effects of the roughness elements (the larger L_C the higher the complexity of the terrain) and a second one, corresponding to the asymptotic roughness length related to the city considered as a whole. In particular, from the analysis of Eq. (11), two asymptotic behaviors can be found for $z_{0L}(z)$: at elevated levels

$$z_{0\infty} = \lim_{z \rightarrow \infty}(z_{0L}) = \lim_{z \rightarrow \infty} \left(\alpha \cdot \exp\left[-\frac{z}{L_C}\right] + \gamma \right) = \gamma \quad (12)$$

and at the surface

$$z_{0S} = \lim_{z \rightarrow 0}(z_{0L}) = \lim_{z \rightarrow 0} \left(\alpha \cdot \exp\left[-\frac{z}{L_C}\right] + \gamma \right) = \alpha + \gamma \quad (13)$$

It is worth noting that the role played by the local length scale can be viewed in terms of an additional contribution to the vertical gradient of wind speed with respect to the classic law where the roughness length is a constant. In fact, taking the derivative with respect to z of Eq. (1), one obtains $du/dz = \partial u / \partial z = u_*/kz$. On the other hand, if $u=u(z,z_{0L})$ one has:

$$\frac{du}{dz} = \frac{\partial u}{\partial z} + \frac{\partial u}{\partial z_{0L}} \frac{dz_{0L}}{dz} \quad (14)$$

where the first term at the right hand side of Eq. (14) is related to the classic form of z_0 . From Eqs. (2) and (10), the additional new term in (14) can be rewritten as:

$$\frac{\partial u}{\partial z_{0L}} \frac{dz_{0L}}{dz} = \beta \frac{u_*}{k} \frac{z_{0L}^{-\gamma}}{z_{0L}} \quad (15)$$

which depends on z , reaching a maximum at low levels and tending to zero at higher heights, where $z_{0L} \rightarrow \gamma$ (see Eq. 12). The importance of this term is weighted by the length scale $L_C = 1/\beta$, which modulates the magnitude of the deviation from the classical log-law. Note that Harman and Finnigan [14], who adopted Physick and Garratt's [28] idea to consider, in the framework of MOST, a function representing the effect of the canopy on the gradient of the wind profile above the canopy, introduced a correction to the similarity relationship for the wind-speed in vegetated canopies by adding a suitable function of height for the vertical flux of horizontal momentum. They have had the merit of introducing a natural form for the vertical profiles within the RSL that overcomes problems with many earlier forms in the literature. Unfortunately, their model does not seem to be easily extendable to urban canopies. The model we propose here solves in a radically different way the same problem by introducing the concept of local length scale.

Non-linear optimization algorithms applied to the vertical profile of z_{0L} for $u_*(z_{ref}) = 0.49 \text{ m s}^{-1}$ (Fig. 2a), in the height range $0.55 < z/H < 11.1$, gives $\alpha = 3.247 \text{ m}$, $\beta = 0.016 \text{ m}^{-1}$ and $\gamma = 0.345 \text{ m}$ (coefficient of variation $R^2 = 0.89$). Since $L_C = \beta^{-1} = 62.5 \text{ m}$, it may be related to the height of the RSL. In fact, the ratio $L_C/H \approx 3.5$ belongs to the range of ratios between the RSL thickness and the building height found in the literature (see for example KR04). Furthermore, this ratio is not far from the lower limit of the range of constant z_{0L} (see Fig. 2a). Regarding γ , its value is close to the values of the roughness length found in descriptive land-use types referred to urban complexes.

Note that Eq. (11) and related parameters should be considered valid only within the RSL and the portion of ISL below $z/H = 11.1$. Preliminary tests suggest that α , β and γ may be defined in terms of both the building height and the friction velocity. A detailed discussion on this subject will be reported elsewhere.

4. The velocity profiles

To support the argument advanced in the previous section, we compare in Fig. 3a the wind velocity profiles obtained substituting Eq. (11) into the canonical log-law (hereinafter NM):

$$u(z) = \frac{u_*}{k} \ln \left[\frac{z}{\alpha \cdot \exp\left[-\frac{z}{L_c}\right] + \gamma} \right] \quad (16)$$

with those calculated by applying other well-known models based on Eq. (1), which use morphometric methods such as those by MGH98 and KR04. Moreover, Eq. (1) is used also with $z_0 = 0.033 \cdot H$ and $d_0 = 0.7 \cdot H$ on the basis of the approach founded on the obstacle height (see GO99). Note that in all those three models u_* is not measured but calculated via best-fitting of the velocity profiles to the Eq. (1). An additional comparison is performed by using the method proposed by CC02, who calculated z_0 and d_0 via best-fitting to the Eq. (1) assuming for u_* values taken from the spatially averaged shear stresses measured in the ISL, the RSL or the whole surface layer. For ease of comparison between different models, only the cases in which u_* is averaged over the whole surface layer (CC02_SL) and that where u_* is measured at $z_{\text{ref}}=10$ m (CC02_zref) will be discussed here. Figure 3a depicts the wind profiles obtained by applying the aforementioned formulations. The velocities in the figure refer to the averages obtained over the same 36 profiles belonging to the interval $|z/L| \leq 0.01$ used to calculate α , β and γ .

The performance of the different models compared is assessed by the reproducibility parameter, RP (which represents the percentage deviation from the observed profile), viz.:

$$\text{RP} = \frac{1}{N_p} \cdot \sum_{N_p} \sum_{z_k=10 \text{ m}}^{z_k=200 \text{ m}} \frac{|u(z_k)_{\text{mod}} - u(z_k)_{\text{obs}}|}{u(z_k)_{\text{obs}}} \quad (17)$$

where $N_p=36$ is the number of profiles. The coefficient of variation, R^2 , is also calculated by imposing the passage through the origin. NM and both the CC02 models show the best performance (Table 1). In particular, NM attains the maximum value of R^2 (0.98), while both the CC02 models display a lower RP. Note that CC02_SL and CC02_zref show very similar performance as a result of the little variation of u_* with height present in their experiment. Finally, it is also of interest that the values of d_0 calculated with both the CC02 models are nearly twice as large as those expected since $d_0 \leq H$.

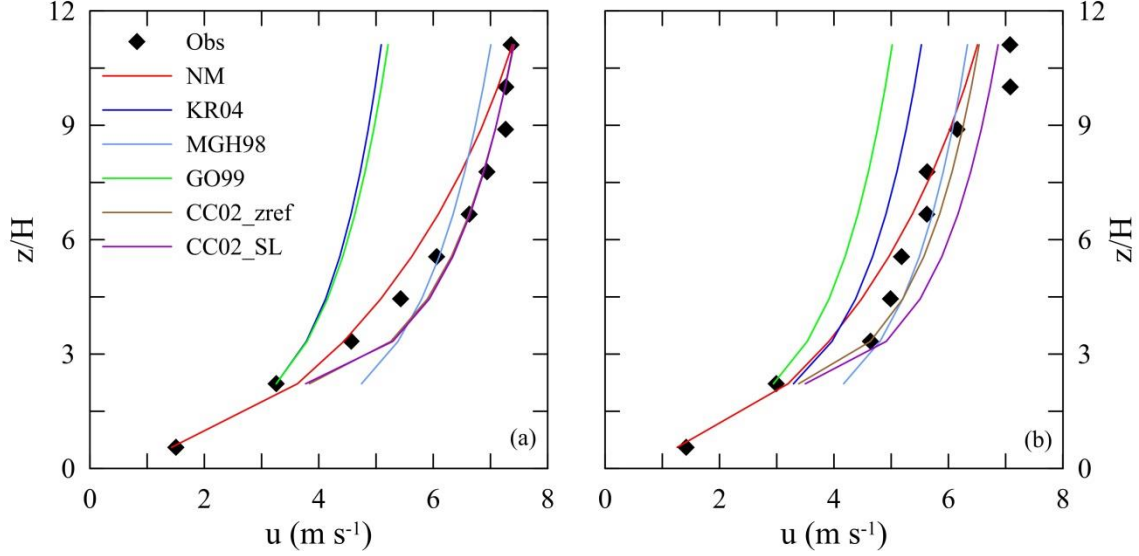


Fig. 3 (a) Vertical profiles of the observed (symbols) and modeled (colored lines) wind velocity for $|z/L| < 0.01$. The profiles are averaged over the 36 events used to calculate the model parameters α , β and γ . (b) As in a), but using the 143 profiles belonging to the interval $0.01 < |z/L| < 0.02$ not used to calculate α , β and γ . Note that in a) the brown line associated with CC02_zref is overlapped by the purple line.

	NM	KR04	MGH98	GO99	CC02_zref	CC02_SL
RP	5.6	29.3	10.3	28.9	5.6	5.5
R²	0.98	0.74	0.34	0.78	0.92	0.91
z₀ (m)	-	1.10	0.53	1.80	0.40	0.29
d₀ (m)	-	16.9	15.1	12.6	30.9	32.6

Table 1 Values of the reproducibility parameter (RP) and the coefficient of variation (R^2) of the wind velocity calculated for each model. α , β and γ and the parameters are calculated for the same interval $|z/L| < 0.01$. The values of z_0 and d_0 are also shown

To test further the model results, we use the same parameters α , β and γ obtained for $|z/L| < 0.01$ to calculate the 143 velocity profiles belonging to the interval of stability $0.01 < |z/L| < 0.02$, which can be considered representative of near-neutral conditions. Those profiles, not used to obtain α , β and γ , are nearly four times the number of profiles considered during the training phase. The results suggest that NM works reasonably well (see Fig. 3b and Table 2), with performance higher than that shown by the other models. Among the classical approaches, the best results are obtained again by CC02_SL, even though the estimated d_0 seems to be too large. Note that all formulations give high correlation coefficients. In contrast, slopes and intercepts given by NM are clearly closer to the optimal values

(respectively 1 and 0) compared to the other models. Therefore, NM simulates adequately not only the vertical trend of the wind velocity but also its absolute value.

	NM	KR04	MGH98	GO99	CC02_zref	CC02_SL
RP	7.5	14.3	9.3	20.9	6.1	9.4
R²	0.97	0.93	0.93	0.94	0.92	0.92
Slope	0.91	0.56	0.54	0.52	0.77	0.81
Intercept (m s⁻¹)	0.14	1.64	2.56	1.38	1.33	1.37

Table 2 Performance of the velocity profiles belonging to the interval $0.01 < |z/L| < 0.02$. The parameters α , β and γ used to calculate the velocity profiles are the same as those calculated by considering the interval $|z/L| < 0.01$

Finally, it is interesting to investigate the role played by the additional term in the velocity gradient relationship (Eq. 14). As is well-known, the MOST is based on the hypothesis that the non-dimensional gradient of the wind-speed:

$$\phi_m = \frac{kz}{u_*} \frac{du}{dz} \quad (18)$$

is unity. In contrast, for the classical log-law (Eq. 1):

$$\phi_m^{CL} = \frac{z}{z-d_0} \quad (19)$$

while for NM:

$$\phi_m^{NM} = 1 + \beta \frac{z_{z0} - \gamma}{z_{0z}} z \quad (20)$$

Figure 4a depicts ϕ_m^{CL} and ϕ_m^{NM} calculated as a function of z/H using the same dataset and all the above-mentioned formulations. Obviously, they all show a strong dependence on z/H .

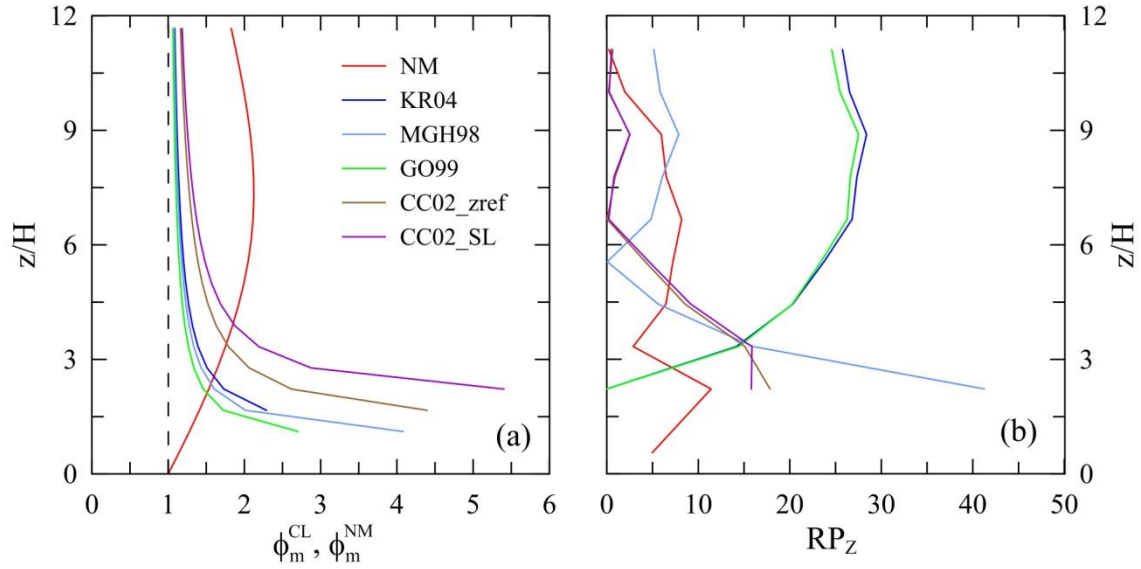


Fig. 4 (a) Non-dimensional velocity gradients ϕ_m^{CL} and ϕ_m^{NM} calculated for all the compared formulations as a function of the non-dimensional height. The dashed line indicates $\phi_m = 1$. (b) As in a) but for RP_Z . All data refer to $N_p=36$

While at elevated heights all the non-dimensional velocity gradients tend to unity, they differ substantially close to the surface in that $\phi_m^{CL} \rightarrow \infty$ for $z \rightarrow d_0$. In contrast, $\phi_m^{NM} \rightarrow 1$ at the surface (as for the MOST) and attains a maximum at $z \cong 2 \cdot L_c \cong 130$ m. In other words, for $z \rightarrow 0$ and $z \rightarrow \infty$ NM shares the same behavior with the MOST (i.e. $\phi_m = 1 \forall z$, dashed line in Fig. 4a), while for intermediate levels the additional term (Eq. 15) acts in modulating the wind velocity to take into account the RSL. This is reflected in the values of RP_Z , that is RP calculated as a function of the height (Fig. 4b). NM shows low RP_Z irrespective of the height, while all formulations based on ϕ_m^{CL} exhibit much more variability of RP_Z ; i.e. low RP_Z at large z/H are accompanied by high RP_Z close to the surface and *vice versa*.

5. Conclusions

In this work we propose a new model to evaluate the wind profiles for neutral conditions in urban areas. We showed that the role played by the roughness length may be taken by a local length scale, z_{0L} , which depends on the altitude. A decrease of z_{0L} with height up to 200 m above the ground was found, which cannot be explained in terms of the (little) vertical variation of u_* that takes place within the same height range. An interpretation of the experimental result is proposed, and a formulation of the local length scale which decays exponentially with height is introduced. The model is based on

three parameters α , L_C and γ to be estimated throughout experimental data. While L_C and γ appear to conform, respectively, to the RSL height and the classic roughness length derived from land-use types referred to urban complexes, the meaning of α is still not clear, except that it might be linked with the local roughness elements. The overall performance of the modeled vertical profiles of the wind velocity is better than that shown by other models that have been proposed in the literature. This is valid also considering vertical velocity profiles referred to near-neutral conditions ($0.01 < |z/L| < 0.02$) adopting the same model parameters calculated for $|z/L| < 0.01$. Finally, the proposed model might pave the way for new formulations of the wind profile also for diabatic conditions.

ACKNOWLEDGEMENTS

We are grateful to Dr. C. Gariazzo for his collaboration during the field campaign.

REFERENCES

- [1] Andreas EL, Claffey KJ, Jordan RE, Fairall CW, Guest PS, Persson POG, Grachev AA (2006) Evaluations of the von Karman constant in the atmospheric surface layer. *J Fluid Mech* 559:117-149.
- [2] Argentini S, Pietroni I, Gariazzo C, Amicarelli A, Mastrantonio G, Pelliccioni A, Petenko I, Viola A (2009) Boundary layer temperature profiles by a RASS and a microwave radiometer: Differences, limits and advantages. *Nuovo Cimento B* 124: 549-564.
- [3] Arya SPS (1975) Buoyancy effects in a horizontal flat-plane boundary layer. *J Fluid Mech* 68:321-343.
- [4] Barlow JF, Rooney GG, von Hünerbein S, Bradley SG (2008) Relating urban surface-layer structure to upwind terrain for the Salford Experiment (Salfex). *Bound-Lay Meteorol* 127:173-191.
- [5] Britter RE, Hanna SR (2003) Flow and dispersion in urban areas. *Annu Rev Fluid Mech* 35:469-496.
- [6] Cheng H, Castro IP (2002) Near wall flow over urban-like roughness. *Bound-Lay Meteorol* 104:229-259.
- [7] Dallman A, Di Sabatino S, Fernando HJS (2013) Flow and turbulence in an industrial/suburban roughness canopy. *Environ Fluid Mech* 13:279-307.
- [8] De Ridder K (2010) Bulk transfer relations for the Roughness sublayer. *Bound-Lay Meteorol* 134:257-267.
- [9] Di Sabatino S, Leo LS, Cataldo R, Ratti C, Britter RE (2010) Construction of digital elevation models for a southern European city and a comparative morphological analysis with respect to northern European and north American cities. *J Appl Meteorol Climatol* 49:1377-1396.
- [10] Fernando HJS (2010) Fluid dynamics of urban atmospheres in complex terrain. *Annu Rev Fluid Mech* 42:365-389.
- [11] Frenzen P, Vogel CA (1995) On the magnitude and apparent range of variation of the von Karman constant in the atmospheric surface layer. *Bound-Lay Meteorol* 72:371-392.
- [12] Garrat JR (1992) *The atmospheric boundary layer*. Cambridge University Press, Cambridge.
- [13] Grimmond CSB, Oke TR (1999) Aerodynamic properties of urban areas derived from analysis of urban surface form. *J Appl Meteorol* 38:1261-1292.
- [14] Harman IN, Finnigan JJ (2007) A simple unified theory for flow in the canopy and roughness sublayer. *Bound-Lay Meteorol* 123:339-363.
- [15] Hertwig D, Efthimiou GC, Bartzis JC, Leitl B (2012) CFD-RANS model validation of turbulent flow in a semi-idealized urban canopy. *J Wind Eng Ind Aerodyn* 111:61-72.
- [16] Karlsson S (1986) The applicability of wind profile formulas to an urban-rural interface site. *Bound-Lay Meteorol* 34:333-355.
- [17] Kastner-Klein P, Rotach MW (2004) Mean flow and turbulence characteristics in an urban roughness sublayer. *Bound-Lay Meteorol* 111:55-84.
- [18] Li QS, Zhi LH, Hu F (2009) Field monitoring of boundary layer wind characteristics in urban area. *Wind Struct* 12:553-574.
- [19] Leuzzi G, Monti P (1997) Breeze Analysis by Mast and Sodar Measurements. *Nuovo Cimento C* 20:343-359.
- [20] Macdonald RW, Griffiths RS, Hall DJ (1998) An Improved Method for the Estimation of Surface Roughness of Obstacle Arrays. *Atmos Environ* 32:1857-1894.
- [21] Monti P, Leuzzi G (2005) A numerical study of mesoscale flow and dispersion over coastal complex terrain. *Int J Environ Pollut* 25 Nos 1/2/3/4:239-250.
- [22] Oke TR (1976) The distinction between canopy and boundary-layer urban heat island. *Atmosphere* 14:268-277.
- [23] Oke TR (1988) *Boundary layer climates*. Routledge, New York.

- [24] Panofsky HA, Dutton JA (1984) *Atmospheric Turbulence*. John Wiley & Sons, New York.
- [25] Pelliccioni A, Monti P, Gariazzo C, Leuzzi G (2012) Some characteristics of the urban boundary layer above Rome, Italy, and applicability of Monin-Obukhov similarity. *Environ Fluid Mech* 12:405-428.
- [26] Pelliccioni A, Monti P, Leuzzi G (2014) Roughness length parameterization in urban boundary layers. *Int J Environ Pollut*, In press.
- [27] Petenko I, Mastrantonio G, Viola A, Argentini S, Coniglio L, Monti P, Leuzzi G (2011) Local circulation diurnal patterns and their relationship with large-scale flows in a coastal area of the Tyrrhenian Sea. *Bound-Lay Meteorol* 139:353-366.
- [28] Physick WL, Garratt JR (1995) Incorporation of a high-roughness lower boundary into a mesoscale model for studies of dry deposition over a complex terrain. *Bound-Lay Meteorol* 74:55-71.
- [29] Pournazeri S, Venkatram A, Princevac M, Tan S, Schulte N (2012) Estimating the height of the nocturnal boundary layer for dispersion applications. *Atmos Environ* 54:611-623.
- [30] Stull RB (1988) *An introduction to Boundary Layer Meteorology*. Kluwer Academic Publisher, Dordrecht.
- [31] Tennekes H (1973) The logarithmic wind profile. *J Atmos Sci* 30:234-238.
- [32] Zilitinkevich SS, Mammarella I, Baklanov AA, Joffre SM (2008) The effect of stratification on the aerodynamic roughness length and displacement height. *Bound-Lay Meteorol* 129:179-190.